Modeling complex intersections with the cell-transmission model

Gunnar Flötteröd [*] Jannis Rohde [†]

July 19, 2009

Report TRANSP-OR 090719
Transport and Mobility Laboratory
Ecole Polytechnique Fédérale de Lausanne
transp-or.epfl.ch

[*]Transport and Mobility Laboratory, Ecole Polytechnique Fédérale de Lausanne, CH-1015 Lausanne, Switzerland, gunnar.floetteroed@epfl.ch (corresponding author)

[†]Institute of Transport, Road Engineering and Planning, Leibniz Universität Hannover, D-30167 Hannover, Germany, rohde@ivh.uni-hannover.de

Abstract

This article widens the scope of the cell-transmission model (CTM) (Daganzo, 1994; Daganzo, 1995a) to the modeling of urban traffic, which is dominated by intersection dynamics. The CTM has originally been proposed for freeways, and it is not immediately applicable to urban traffic for the following reasons: Its intersection model is limited to three-legged topologies and ignores all stream line interactions apart from pure inflow capacity constraints of downstream merges, and, like every first order model, the CTM does not impose limits on vehicle accelerations and decelerations. However, the CTM has a number of important advantages that motivate an effort to carry it over to urban traffic instead of setting up an entirely new model: It is computationally efficient, requires only few, intuitive parameters, and, last but not least, it is well-understood by both researchers and practitioners.

The realistic modeling of urban traffic with the CTM requires to specify the model for arbitrary intersection topologies without affecting its basic principles and to incorporate additional flow constraints that capture stream line interactions within intersections. The model's infinite accelerations are an intrinsic property of all first order models, and hence it appears more plausible to milden their negative effects by appropriate parametrization instead of attempting to move the CTM out of this model class. Finally, a framework is desirable that allows for incremental phenomenological modeling based on a basic specification of greatest generality. This article treats all of these issues in detail and demonstrates that the CTM is applicable to the modeling of complex urban intersections.

1 Introduction

Traffic flow models describe vehicular dynamics given a certain traffic infrastructure and, if applicable, given additional route and destination choice information. The infrastructure comprises the considered road (system) in terms of geometry, speed limits, and such. If a complete network is given, this also includes intersection properties such as turning move limitations, right-of-way laws, and signaling, and it requires supplementary route

and destination choice information. The vehicular dynamics may be described at various levels of details, ranging from single-vehicle interactions ("car-following models"), e.g., (Brackstone & McDonald, 1999; Pandawi & Dia, 2005), over partially aggregate ("mesoscopic") models, e.g., (Astarita et al., 2001; Ben-Akiva et al., 2001; De Palma & Marchal, 2002; Mahmassani, 2001; Nökel & Schmidt, 2002), to fully macroscopic models that treat vehicular traffic flows as continuous streams. The latter model class is considered in this article. The major advantage of macroscopic models is their convenient mathematical structure and their relatively low number of parameters.

Macroscopic models for traffic flow on a link have gone from the fundamental diagram (where density and velocity are uniquely related and flow is a function of either density or velocity (Greenshields, 1935)) via the Lighthill-Whitham-Richards theory of kinematic waves (where the fundamental diagram is inserted into an equation of continuity (Lighthill & Witham, 1955; Richards, 1956)) to second-order models (where a second equation introduces inertia (Payne, 1971)). In this article, we concentrate on the kinematic wave model (KWM), and we assertively refrain from joining the ongoing debate if more complex models yield a substantial gain in expressive power, e.g., (Hoogendoorn & Bovy, 2001; Nagel & Nelson, 2005).

Instances of the KWM are collectively referred to as "first order models" because they model velocity (first order information) but do not explicitly specify an acceleration/deceleration law (which would constitute second order information). Macroscopic first order models capture a bird's view on traffic flow: They do not distinguish individual vehicles, and they allow arbitrarily abrupt velocity changes; both features are consistent with empirical evidence only if sufficiently large space- and time-scales are considered. These properties of the KWM apply well to freeway traffic but are more difficult to associate with urban traffic. The objective of this work is to widen the scope of (a particular instance of) the KWM to the modeling of urban traffic.

Specifically, we consider the cell-transmission model (CTM) (Daganzo, 1994; Daganzo, 1995a; Daganzo, 1995b), which is arguably the most popular instance of the KWM. It is closely related to the STRADA model (Buisson et al., 1996a; Buisson et al., 1996b) in that both implement the Godunov scheme, which is a numerical solution procedure that applies to the KWM

in a particularly intuitive way (Lebacque, 1996; LeVeque, 1992), which is described further below. The CTM has found various applications, e.g., in freeway ramp metering, signal optimization, and traffic state estimation (Friedrich & Almasri, 2006; Feldman & Maher, 2002; Sun et al., 2003; Tampere & Immers, 2007), and has been subject to thorough experimental validations, e.g., (Brockfeld & Wagner, 2006; Munoz et al., 2006; Munoz et al., 2004). Most attention, however, has been paid to its application for the modeling of freeway traffic.

In this article, it is demonstrated that, with appropriate extensions, the CTM is also applicable to the modeling of urban traffic. Apart from their generally smaller time scales when compared to freeways, urban traffic flows are dominated by intersection dynamics. Also, because vehicle velocities in urban networks are relatively low, certain intersection conflicts can be safely resolved based on right-of-way laws that go without explicit signaling. Hence, the adequate modeling of urban traffic requires to also represent this type of intersections within the CTM. Early work that aims in this direction is (Lee, 1996; Ziliaskopoulos & Lee, 1997). However, this model relies on a sole recombination of existing CTM building blocks and applies only to signalized intersections.

A more general perspective is adopted in (Lebacque, 1996; Lebacque & Koshyaran, 2002), where various first order models are discussed within a unified demand/supply framework. This framework enables the aforementioned intuitive solution of the Godunov scheme. Essentially, it states that traffic flows are invariably maximized subject to phenomenological constraints on upstream outflows (flow demands) and downstream inflows (flow supplies) at all locations in the network, including intersections.

A recent proposal along these lines is (van Hinsbergen et al., 2009), which captures stream line interactions within an intersection by imposing additional phenomenological constraints on the flow maximization of the demand/supply framework. While our article treats a related topic, it stands out from van Hinsbergen et al. (2009) in the following aspects.

1. We base our work on the established phenomenology of the CTM. This model constitutes an extreme case of a first order model in that it disregards all flow interactions that may occur within an intersection: If a vehicle (unit) is ready to depart from an upstream link and

if there is sufficient space on a downstream link, this vehicle (unit) is always transmitted. While this phenomenology alone is clearly inappropriate to model a complex urban intersection, its constitutes a very unrestricted base model on top of which further flow constraints can be imposed, if necessary. That is, since the CTM exhibits extremely weak flow constraints, it introduces only a minimum of phenomenological a priori assumptions in a more case-specific intersection model with additional constraints.

2. In order to apply the CTM as a base model for urban intersections, its phenomenology is adopted to intersections of arbitrary topology. The difficulty of extending the CTM in this regard has been well recognized in the literature (Jin & Zhang, 2003). We present a straightforward generalization of the CTM's flow transmission rules that applies to intersections of general topology. This generalization exhibits the same extreme flow transmissions as the original CTM and relies on the same small set of parameters. This is a continuation of work originally presented in (Flötteröd & Nagel, 2005; Flötteröd, 2008).

3. Regarding the introduction of additional phenomenological intersection flow constraints, our work substantially generalizes (van Hinsbergen et al., 2009) in that we model these constraints as functions of the *actual flows* in the intersection and not, like van Hinsbergen et al. (2009), as functions of the *greatest possible inflows*. The latter approach can lead to unrealistic results when possible inflows are held back because of, e.g., spillback from a downstream merge or further flow interactions within the intersection. The applicability of our approach, which properly accounts for the actual conditions within an intersection, is not constrained to the CTM and applies to arbitrary intersection models that implement the demand/supply framework.

4. The uniqueness of intersection flows under additional flow constraints is investigated. It turns out that (i) flows in point-like intersection models can be non-unique even for simple three-armed topologies and (ii) problems of this kind are likely to result from parameter misspecifications in combination with the limitations of the point-like modeling approach as such. This analysis indicates that intersections beyond a certain spatial complexity should indeed be modeled spatially,

at least by distinguishing several point-like intersection elements.

The remainder of this article is organized as follows. Section 2 provides a brief introduction to the KWM and the demand/supply framework, which underlie the CTM. Section 3 revisits the CTM's flow transmission rules and generalizes them for intersections of arbitrary topology. Section 4 enhances this model with additional flow constraints. Both Section 3 and 4 are supported by experimental results. Finally, Section 5 concludes the article.

2 Foundations of the cell-transmission model

The CTM is an instance of the KWM. The KWM requires a minimal set of assumptions to model traffic flow on a linear road. Denote by $x \in \mathbb{R}$ a location on that road and by $t \in \mathbb{R}$ the continuous time. $\rho(x,t)$ is the local density (in vehicle units per length unit) of traffic, $q(x,t)$ is its flow (in vehicle units per time unit), and $v(x,t)$ is its velocity. These quantities are related by the first constituent equation of the KWM:

$$q(x,t) = v(x,t)\rho(x,t). \tag{1}$$

The second modeling assumption is that of vehicle conservation. On smooth conditions, it is expressed by the continuity equation

$$\frac{\partial \rho}{\partial t} + \frac{\partial q}{\partial x} = 0. \tag{2}$$

Finally, local flow is specified as a function of local density only. This relation is usually denoted as the fundamental diagram:

$$q(x,t) = Q(\rho(x,t), x). \tag{3}$$

Since these specifications can still result in ambiguities, an additional condition must be instrumented to select the physically relevant solution. Given a concave fundamental diagram, the principle of local demand and supply provides a convenient technique to ensure uniqueness (Lebacque, 1996). Technically, this constitutes an instance of the Godunov scheme. Denote by $x-$ ($x+$) the location immediately upstream (downstream) of x. For

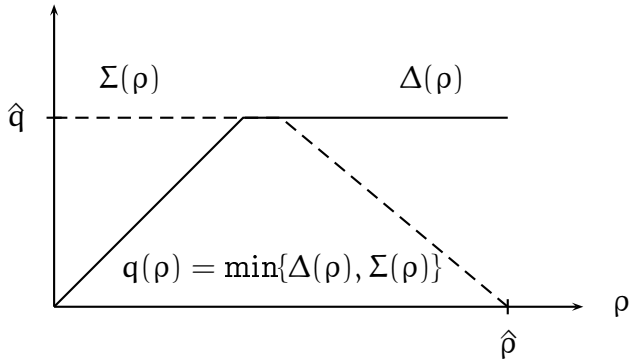

Figure 1: Local demand and supply comprise a fundamental diagram
The piecewise linear demand function $\Delta(\rho)$ (solid) conforms to the original specification of the CTM, where it is denoted as the sending function. It consists of an increasing part with its slope equal to the free flow speed, and it is limited by the flow capacity $\hat{q}$. The supply function $\Sigma(\rho)$ (dashed; also consistent with the CTM, where it is called receiving function) is also limited by the flow capacity. The slope of its declining part equals the backward wave speed and intersects the abscissa at the greatest possible density $\hat{\rho}$. The minimum of both functions yields a fundamental diagram. Piecewise linearity is a particular property of the CTM. The demand/supply framework applies more generally to concave demand and supply functions.

every x, the local flow $q(x,t)$ is then defined as the minimum of local **flow demand** $\Delta(\rho(x-,t),x-)$ and local **flow supply** $\Sigma(\rho(x+,t),x+)$:

$$q(x,t) = \min\{\Delta(\rho(x-,t),x-), \Sigma(\rho(x+,t),x+)\}. \tag{4}$$

Figure 1 illustrates this function. The CTM adheres to this specification, given piecewise linear demand and supply functions.

To begin with, (4) reflects the self-evident constraint that local traffic flow is bounded by the flow that can be dismissed from the immediate upstream location and by the flow that can be absorbed by the immediately downstream location. But furthermore, the local flow is maximized subject to these constraints. This property enforces the physically relevant solution of the KWM. Phenomenologically, it is a statement of drivers' ride impulse (Ansorge, 1990), which is equivalently expressed by the microsimulation

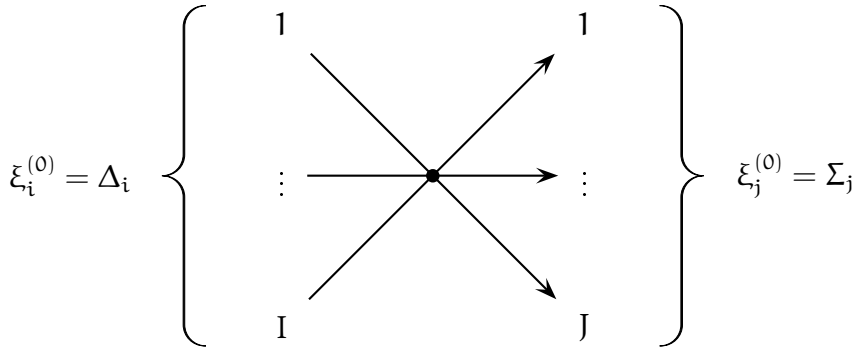

Figure 2: A general intersection with I ingoing and J outgoing links
The mapping of upstream demands Δ and downstream supplies Σ on initial resources $\xi^{(0)}$ is specified in (5).

rule for cellular automata "Drive as fast as you can and stop if you have to!" (Chrobok et al., 2003; Daganzo, 2006).

Beyond its ability to uniquely capture traffic flow along a link, this principle also holds for the modeling of general intersections, cf. Figure 2. In such a setting, every upstream link i provides a demand $\Delta_i(t)$ equal to its greatest possible outflow towards the intersection, and every downstream link j provides a supply $\Sigma_j(t)$ equal to its greatest possible inflow. Additional phenomenological modeling is facilitated since these boundaries alone are generally not sufficient to uniquely define all flows across the intersection. However, every reasonable specification must adhere to the principle of local flow maximization subject to all phenomenological constraints.

3 General intersection topologies

The extended CTM for general intersections (ECTM) is developed in two steps. First, the structural workings of the original CTM are revisited in Section 3.1. Second, these workings are formally generalized and mapped on intersections of arbitrary topology in Section 3.2. The resulting specification is illustrated with an example in Section 3.3.

The CTM is consistent with the demand/supply framework of Lebacque

(1996) in that it maximizes all flow transmissions subject to a set of phenomenological constraints. Even within this class of models, the CTM constitutes an extreme instance in that it transmits all upstream flow demands that face sufficient flow supplies on their downstream links. As stated in the introduction, this is likely to overestimate the actual flows in urban intersections, where vehicle interactions within the intersection further constrain the flow throughput.

However, the general modeling approach proposed here is of an incremental nature in that it relies on a base model that exhibits flow constraints that are as weak as possible. This provides convenient flexibility in the modeling of particular intersections by adding further phenomenological constraints only when necessary. The weak flow constraints of the CTM make it highly suitable as a such a base model.

3.1 The cell-transmission model revisited

The CTM runs in discrete time and space. Its spatial discretization units are denoted as cells. The CTM specifies the transmission of real-valued vehicle units in three possible cell configurations: (i) linear connection of one upstream cell and one downstream cell, (ii) diverge with one upstream cell and two downstream cells, and (iii) merge with two upstream cells and one downstream cell.

The amount of vehicles that is transmitted in a single simulation time step is computed in one (linear, diverge) or two (merge) **stages**, and vehicles are transmitted in fixed proportions from the upstream cell(s) to the downstream cell(s) in every stage. Since the notions of "transmitted vehicles" and "transmitted flows / flow rates" (in vehicles per time unit) differ only by a proportionality constant that depends on the simulation time step length, the model is from now on expressed in terms of flow rates only.

In detail, the CTM specifies the following flow transmission rules.

- The **linear flow transmission rule** consists of a single stage. It states that the amount of transmitted flow is maximized subject to the following constraints:
  - The transmitted flow must note exceed the flow demand in the upstream cell.

- The transmitted flow must not exceed the flow supply in the downstream cell.

- The **diverge flow transmission rule** also consists of a single stage. It states that the amount of transmitted flow is maximized subject to the following constraints:

  - The transmitted flow must not exceed the flow demand in the upstream cell.
  - The outflow of the upstream cell is split according to exogenously specified turning fractions.
  - The inflow of each downstream cell, which is equal to the upstream outflow multiplied by the according turning fraction, must not exceed the flow supply in that downstream cell.

  This specification is consistent with a first in/first out (FIFO) assumption on the upstream link.

- The **non-congested merge flow transmission rule** applies if the sum of flow demands in the upstream cells does not exceed the flow supply in the downstream cell. This rule consists of a single stage. It states that both upstream cells transmit all of their available flows.

- The **congested merge flow transmission rule** applies if the total flow demand in the upstream cells exceeds the available space in the downstream cell. This rule consists of two stages. In the first stage, the inflow of the downstream cell is maximized subject to the following constraints:

  - The outflow of either upstream cell must not exceed the flow demand in that cell.
  - The upstream cells transmit flows in a ratio that results from exogenously specified priority parameters.
  - The transmitted flow must not exceed the flow supply in the downstream cell.

  If after the first stage some flow supply remains in the downstream cell then there is at most one upstream cell with a positive flow demand

left. The second stage then consists of an application of the linear flow transmission rule only to this upstream cell and the downstream cell.

These phenomenological rules are now formalized in a way that carries over to intersections of general topology. The multi-stage calculation structure, which ensures that the downstream supplies are used up to the greatest possible extent, is preserved as well as the proportionality of flow transmissions within each stage, which is parametrized only through turning fractions and priority values.

3.2 CTM-consistent specification of general intersections

To begin with, two terms are introduced.

Resources. The CTM's flow calculation logic requires the specification of the maximum flow that can be dismissed from an upstream cell and the maximum flow that can be received by a downstream cell. Here, these demands and supplies are collectively referred to as resources, which are used up during the stage-by-stage flow transmissions of a simulation step.

Consumption rates. The constant ratio according to which resources are used up during a single stage is specified through the ratio of so-called consumption rates. The ECTM is specified such that the resources are "consumed" according to consumption rates the ratio of which is consistent with the original CTM's logic.

In the ECTM's formal generalization of the CTM, flow transmissions are calculated in a multi-stage process with stage index $k = 0 \ldots K$. Every element $\xi_i^{(k)}$ of the resource vector $\boldsymbol{\xi}^{(k)} = (\xi_i^{(k)})$ corresponds at $k = 0$ either to the flow demand in an upstream cell or to the flow supply in a downstream cell:

$$\begin{array}{rcll} \xi_i^{(0)} & = & \Delta_i & \text{for } i \text{ upstream} \\ \xi_j^{(0)} & = & \Sigma_j & \text{for } j \text{ downstream,} \end{array} \tag{5}$$

cf. Figure 2.

These resources are consumed during the process. For any resource i, corresponding either to an upstream or a downstream cell, its rate of consumption in stage k is denoted by $\varphi_i^{(k)}$. (CTM-consistent values for these

parameters are given at the end of this section.) The consumption rate vector $\boldsymbol{\varphi}^{(k)} = (\varphi_i^{(k)})$ alone only specifies the ratios of resource consumptions. To identify the total level of consumption, a "duration" parameter $\theta^{(k)}$ is calculated in every stage k that defines the following resource dynamics:

$$\boldsymbol{\xi}^{(k+1)} = \boldsymbol{\xi}^{(k)} - \theta^{(k)}\boldsymbol{\varphi}^{(k)}. \tag{6}$$

The duration $\theta^{(k)}$ of stage k is such that it reproduces the CTM logic, which transmits as much flow as possible until an upstream cell runs out of flow demand or a downstream cell runs out of flow supply. For this purpose, denote by

$$D^{(k)} = \{i;\, \xi_i^{(k)} > 0\} \tag{7}$$

the set of all resources that are strictly positive at the beginning of stage k. The duration $\theta^{(k)}$ of stage k is then chosen such that the stage ends when the first resource in $D^{(k)}$ reaches a zero value. That is,

$$\theta^{(k)} = \min_{i \in D^{(k)}} \{\xi_i^{(k)}/\varphi_i^{(k)}\}. \tag{8}$$

The consumption rates of stage k only depend on the set $D^{(k)}$ of available resources but not on their levels such that $\boldsymbol{\varphi}^{(k)} = \boldsymbol{\varphi}(D^{(k)})$. This is consistent with the CTM, which defines constant flow transmission ratios within every stage. The process terminates when all consumption rates are zero. The transmitted outflow rates q_i^{out} of upstream cells i and the inflow rates q_j^{in} of downstream cells j then result from

$$\begin{array}{lcll} q_i^{out} & = & \xi_i^{(0)} - \xi_i^{(K)} & \text{for } i \text{ upstream} \\ q_j^{in} & = & \xi_j^{(0)} - \xi_j^{(K)} & \text{for } j \text{ downstream.} \end{array} \tag{9}$$

The resource consumption logic is summarized in Algorithm 1. Note that the temporal aspect of this process is not to be interpreted physically. Only its final state is of relevance to the physical simulation.

The original CTM flow calculation rules and their continuation into a general intersection model can now be expressed by appropriate specifications of the resource consumption rates. The CTM has two types of exogenously specified parameters that affect the flow transmissions and, hence, the consumption rates: priorities and turning fractions. The priority of an upstream cell i is denoted by α_i and the turning fraction from an upstream cell i to a downstream cell j is denoted by β_{ij}.

Algorithm 1 Resource consumption in the ECTM

1. $\boldsymbol{\xi}^{(0)}$ is given
2. $k = 0$
3. $D^{(k)} = \{i;\, \xi_i^{(k)} > 0\}$
4. while $(\boldsymbol{\varphi}(D^{(k)}) \neq \mathbf{0})$, do
   (a) $\theta^{(k)} = \min_{i \in D^{(k)}} \{\xi_i^{(k)} / \varphi_i(D^{(k)})\}$
   (b) $\boldsymbol{\xi}^{(k+1)} = \boldsymbol{\xi}^{(k)} - \theta^{(k)} \boldsymbol{\varphi}(D^{(k)})$
   (c) $D^{(k+1)} = \{i;\, \xi_i^{(k+1)} > 0\}$
   (d) increase k by one
5. $K = k$

Let the consumption rate of upstream resource i be $\varphi_i(D) = \alpha_i$ if both i and all downstream resources towards which i has a non-zero turning fraction are nonzero (i.e., contained in D). This guarantees that the available upstream resources are consumed in ratios that correspond to their priorities, just like in the original CTM. If i has a non-zero turning fraction towards a zero downstream resource, $\varphi_i(D)$ is set to zero. This ensures that all upstream cells are modeled as single-lane roads that block as soon as one relevant downstream cell becomes unavailable.[1]

Consistency with the flow splitting rule of the CTM diverge is maintained by defining consumption rates $\varphi_j(D) = \sum_i \beta_{ij} \varphi_i(D)$ for all downstream resources j. This guarantees both flow conservation and reproduction of the

[1] Further phenomenological modeling is possible within the frame of this specification. Consider several upstream cells i that faces several downstream cells j. One could postulate an individual priority α_{ij} for each i and j. The priorities α_i would then represent an "upstream view" of this configuration. For example, if one wants to enforce the original CTM's logic individually on all merges, one would have to require that $\beta_{i_1 j} \varphi_{i_1} / \beta_{i_2 j} \varphi_{i_2} = \alpha_{i_1 j} / \alpha_{i_2 j}$ holds for all combinations of upstream cells i_1 and i_2, which would (maintaining $\varphi_i = \alpha_i$) imply $\alpha_i = \alpha_{ij} / \beta_{ij}$ for all i and j – clearly an over-specified model. An alternative would be to let $\alpha_i = \min_j \{\alpha_{ij} / \beta_{ij}\}$. We leave the investigation of these phenomenological issues to further experimental studies.

turning fractions. Summarizing, the following resource consumption rates generate flow transmissions that reproduce the CTM's phenomenology:

$$\begin{aligned} \varphi_i(D) &= \begin{cases} \alpha_i & \text{if } i \in D, \{j : \beta_{ij} > 0\} \subseteq D \\ 0 & \text{otherwise} \end{cases} && \text{for } i \text{ upstream} \\ \varphi_j(D) &= \sum_i \beta_{ij} \varphi_i(D) && \text{for } j \text{ downstream,} \end{aligned} \tag{10}$$

where the index set D contains all non-zero resources, cf. (7).

This specification comprises all original CTM intersections, which can be checked by by choosing $I = 1$, $J = 1$ (straight cell connection), $I = 1$, $J = 2$ (diverge connection) or $I = 2$, $J = 1$ (merge connection) and evaluating the resulting stage sequences of resource transmissions (Flötteröd, 2008). For more general intersections, further consistency with the CTM is maintained in that all downstream supplies are invariably used up to the greatest possible extend. This property results from the design of Algorithm 1, which maximizes all flow transmissions subject to the CTM's multi-stage structure, where flows are transmitted in constant ratios in every stage. These ratios are consistent with the original CTM's phenomenology.

The following section clarifies the workings of this model through an example.

3.3 Example

The considered test network is shown in Figure 3. It will be reconsidered in later parts of this article, where the ECTM is compared to a detailed traffic microsimulator. This section only demonstrates the ECTM's workings.

The network consists of a major street in north/south direction, which is intersected by a minor one way street that runs from east to west. Within the ECTM, this network is represented by a single cell intersection with three upstream cells P_S, P_E, P_N and three downstream cells S_N, S_W, S_S. Traffic coming from the south enters the intersection from predecessor cell P_S, traffic coming from the east enters it via P_E, and traffic coming from the north enters it via P_N. The cells S_N, S_W, and S_S represent the northbound, westbound, and southbound exit of the intersection, respectively. 50 percent of the traffic coming from P_S turn left at the intersection, and 50

Table 1: Uncongested flow transmissions

	P_S	P_E	P_N	S_N	S_W	S_S
$\xi^{(0)}$, cf. (5)	600	100	600	1400	1400	1400
$\varphi^{(0)}$, cf. (10)	1	0.1	10	0.5	5.6	5
$\xi^{(0)}/\varphi^{(0)}$	600	1000	60	2800	250	280
$\theta^{(0)}$, cf (8)	60					
$\xi^{(1)}$, cf. (6)	540	94	0	1370	1064	1100
$\varphi^{(1)}$	1	0.1	0	0.5	0.6	0
$\xi^{(1)}/\varphi^{(1)}$	540	940	%	2740	1773.33	∞
$\theta^{(1)}$	540					
$\xi^{(2)}$	0	40	0	1100	740	1100
$\varphi^{(2)}$	0	0.1	0	0	0.1	0
$\xi^{(2)}/\varphi^{(2)}$		400	%	∞	7400	∞
$\theta^{(2)}$	400					
$\xi^{(3)}$	0	0	0	1100	700	1100
$\varphi^{(3)}$	0	0	0	0	0	0

Workings of the ECTM in uncongested conditions. Every block of rows represents one flow transmission stage. The algorithm terminates when all resource consumptions have ceased. The simulated flow rates are, according to (9), $q_S^{out} = 600\,\text{veh/h}$, $q_E^{out} = 100\,\text{veh/h}$, $q_N^{out} = 600\,\text{veh/h}$, $q_N^{in} = 300\,\text{veh/h}$, $q_W^{in} = 700\,\text{veh/h}$, and $q_S^{in} = 300\,\text{veh/h}$.

percent of the traffic coming from P_N turn right at the intersection, both into successor cell S_W. The traffic on the minor street only crosses the intersection. Summarizing, $\beta_{SN} = 0.5$, $\beta_{SW} = 0.5$, $\beta_{EW} = 1$, $\beta_{NW} = 0.5$, and $\beta_{NS} = 0.5$. The right-of-way laws at the westbound merge S_W are modeled through the priority values $\alpha_N = 10$, $\alpha_S = 1$, and $\alpha_E = 0.1$. The further parameters of this intersection are described later in Section 4.4, where they become relevant for the first time.

Consider first an uncongested scenario, where the supplies of all downstream cells are sufficient to absorb all upstream demands. In particular, the following flow demand and supply values are assumed: $\Delta_S = 600\,\text{veh/h}$, $\Delta_E = 100\,\text{veh/h}$, $\Delta_N = 600\,\text{veh/h}$, $\Sigma_N = 1400\,\text{veh/h}$, $\Sigma_W = 1400\,\text{veh/h}$, and $\Sigma_S = 1400\,\text{veh/h}$. Table 1 details the resource consumption process of the

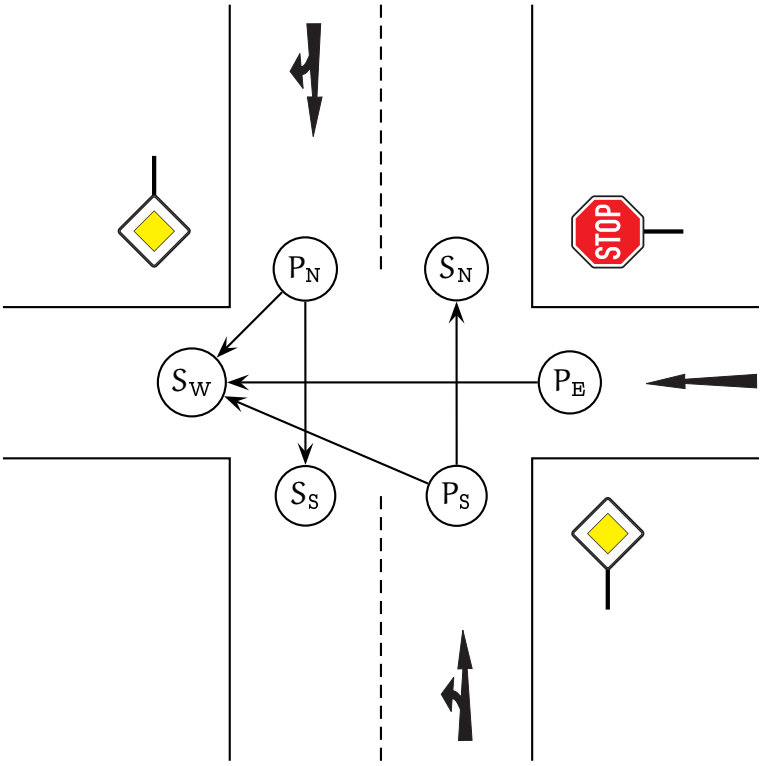

Figure 3: Test network

The network consists of a major street in north/south direction, which is intersected by a minor one way street that runs from east to west. Within the ECTM, this network is represented by a single cell intersection with three upstream cells P_S, P_E, P_N and three downstream cells S_N, S_W, S_S. Traffic coming from the south enters the intersection from predecessor cell P_S, traffic coming from the east enters it via P_E, and traffic coming from the north enters it via P_N. The cells S_N, S_W, and S_S represent the northbound, westbound, and southbound exit of the intersection, respectively. 50 percent of the traffic coming from P_S turn left at the intersection, and 50 percent of the traffic coming from P_N turn right at the intersection, both into successor cell S_W. The traffic on the minor street only crosses the intersection. Summarizing, $\beta_{SN} = 0.5$, $\beta_{SW} = 0.5$, $\beta_{EW} = 1$, $\beta_{NW} = 0.5$, and $\beta_{NS} = 0.5$. The right-of-way laws at the westbound merge S_W are modeled through the priority values $\alpha_N = 10$, $\alpha_S = 1$, and $\alpha_E = 0.1$.

Table 2: Congested flow transmissions

	P_S	P_E	P_N	S_N	S_W	S_S
$\xi^{(0)}$	600	100	600	1400	400	1400
$\varphi^{(0)}$	1	0.1	10	0.5	5.6	5
$\xi^{(0)}/\varphi^{(0)}$	600	1000	60	2800	71.43	280
$\theta^{(0)}$	60					
$\xi^{(1)}$	540	94	0	1370	64	1100
$\varphi^{(1)}$	1	0.1	0	0.5	0.6	0
$\xi^{(1)}/\varphi^{(1)}$	540	940	%	2740	106.67	∞
$\theta^{(1)}$	106.67					
$\xi^{(2)}$	433.33	83.33	0	1316.67	0	1100
$\varphi^{(2)}$	0	0	0	0	0	0

Workings of the ECTM in congested conditions. Every block of rows represents one flow transmission stage. The algorithm terminates when all resource consumptions have ceased. The simulated flow rates are, according to (9), $q_S^{out} = 166.67\,\text{veh/h}$, $q_E^{out} = 16.67\,\text{veh/h}$, $q_N^{out} = 600\,\text{veh/h}$, $q_N^{in} = 83.33\,\text{veh/h}$, $q_W^{in} = 400\,\text{veh/h}$, and $q_S^{in} = 300\,\text{veh/h}$.

ECTM in these conditions. Every block of rows in this table corresponds to one stage of the ECTM. All upstream demands are fully served by the model: The simulated flow rates are, according to (9), $q_S^{out} = 600\,\text{veh/h}$, $q_E^{out} = 100\,\text{veh/h}$, $q_N^{out} = 600\,\text{veh/h}$, $q_N^{in} = 300\,\text{veh/h}$, $q_W^{in} = 700\,\text{veh/h}$, and $q_S^{in} = 300\,\text{veh/h}$. The need to evaluate more than a single stage of the ECTM results from the fact that a new stage starts every time a resource runs dry, even if it is an upstream resource in uncongested conditions. All upstream cells' outflows are split proportionally to their respective turning fractions.

The flow interactions are more complex when the demand exceeds the supply such that congestion occurs. The following values represent a congested scenario: $\Delta_S = 600\,\text{veh/h}$, $\Delta_E = 100\,\text{veh/h}$, $\Delta_N = 600\,\text{veh/h}$, $\Sigma_N = 1400\,\text{veh/h}$, $\Sigma_W = 400\,\text{veh/h}$, and $\Sigma_S = 1400\,\text{veh/h}$. The total demand for S_W is $\beta_{SW}\Delta_S + \beta_{EW}\Delta_E + \beta_{NW}\Delta_N = 700\,\text{veh/h}$, which exceeds its supply of 400 veh/h. Table 2 details how this situation is simulated in the ECTM. In stage 0, all resources are available, all upstream resources are used up pro-

portionally to their priorities, and all downstream resources are consumed by inflows that result from weighting the upstream transmissions with the turning fractions. The upstream resource P_N, which has the highest priority and hence the highest consumption rate, runs dry most quickly. Next, the downstream resource S_W runs dry in stage 1. Since all upstream cells have a non-zero turning fraction towards this resource, all resource consumptions cease in stage 2 such that the algorithm terminates. The simulated flow rates are, according to (9), $q_S^{out} = 166.67\,\text{veh/h}$, $q_E^{out} = 16.67\,\text{veh/h}$, $q_N^{out} = 600\,\text{veh/h}$, $q_N^{in} = 83.33\,\text{veh/h}$, $q_W^{in} = 400\,\text{veh/h}$, and $q_S^{in} = 300\,\text{veh/h}$. These results exhibit the following features:

- All flow transmissions are proportional to their respective turning fractions;
- the FIFO property is obeyed in that every upstream cell that has at least one unavailable downstream cell transmits no further flows;
- the flow from P_N is completely transmitted because its priority is high enough to reserve sufficient capacity in S_W. The remainder of S_W's capacity is completely used up by P_S and P_E, the outflows of which are proportional to their priorities.

These experiments show how the ECTM maintains consistency with the original CTM's modeling assumptions while at the same time disposing of its topology constraints. However, the ability to model complex intersections also introduces new difficulties: Conflicting stream lines (in this example: the left- turning portion of the northbound flow vs. the southbound flow and the minor flow vs. all major flows) are not yet accounted for. The following section shows how they can be consistently incorporated in the model.

4 Endogenous capacity constraints

Endogenous capacity constraints model situations where the interactions of traffic streams within an intersection reduce its throughput. This does not comprise the basic upstream outflow and downstream inflow constraints, which depend on the states of adjacent links and hence are exogenous from the intersection's perspective.

Section 4.1 adds endogenous capacity constraints to the simulation logic of the ECTM while maintaining consistency with the underlying demand/supply framework. Section 4.2 discusses specification and uniqueness issues. Section 4.3 presents two solution procedures for the model, and Section 4.4 compares the endogenously constrained ECTM with a detailed traffic microsimulator.

4.1 Specification

Speaking in terms of the ECTM, the simulation of a complex intersection implies, in every time step, the mapping of upstream demands $\boldsymbol{\Delta} = (\Delta_i)$ and downstream supplies $\boldsymbol{\Sigma} = (\Sigma_j)$ on an initial resource vector $\boldsymbol{\xi}^{(0)}$, which is then consumed in K stages into a final resource vector $\boldsymbol{\xi}^{(K)}$, from which an intersection flow rate vector is obtained that equals the amount of consumed resources, cf. (5), Algorithm 1, and (9). These calculations constitute the simulation map

$$\mathbf{q} = \begin{pmatrix} \mathbf{q}^{\text{out}} \\ \mathbf{q}^{\text{in}} \end{pmatrix} = \text{sim}(\boldsymbol{\Delta}, \boldsymbol{\Sigma}) \tag{11}$$

where $\mathbf{q}^{\text{out}} = (q_i^{\text{out}})$ is a I-dimensional vector of upstream outflows and $\mathbf{q}^{\text{in}} = (q_j^{\text{in}})$ is a J-dimensional vector of downstream inflows.

The endogenous capacity constraints are specified for the outflows of upstream cells only. This is no confinement because of the model's FIFO property: Actual constraints apply to individual traffic streams, so there is possibly more than one constraint affecting the outflow of an upstream cell. However, since all outflows of this cells are coupled by the FIFO rule, these constraints can be combined in a single outflow constraint. The constraints are enforced by a **demand constraint function** $\widehat{\boldsymbol{\Delta}}(\mathbf{q})$ that bounds the original demand $\boldsymbol{\Delta}$ given a flow pattern $\mathbf{q}$ in the intersection. The suchlike constrained demands $\boldsymbol{\Delta}(\mathbf{q})$ result from

$$\boldsymbol{\Delta}(\mathbf{q}) = \min\{\boldsymbol{\Delta}, \widehat{\boldsymbol{\Delta}}(\mathbf{q})\}, \tag{12}$$

where the min function applies element by element.

The endogenously constrained simulation problem thus requires to identify flow rates $\mathbf{q}$ that solve the fixed-point problem

$$\begin{aligned} \mathbf{q} &= \text{sim}(\boldsymbol{\Delta}(\mathbf{q}), \boldsymbol{\Sigma}) \\ &= \text{sim}(\min\{\boldsymbol{\Delta}, \widehat{\boldsymbol{\Delta}}(\mathbf{q})\}, \boldsymbol{\Sigma}). \end{aligned} \tag{13}$$

This does not affect the ECTM's consistency with the original CTM. It only introduces additional phenomenological constraints into the underlying demand/supply framework. Consequently, this specification can be applied to any intersection model that is based on this framework.

A solution of model (13) is guaranteed if the demand constraint function $\widehat{\boldsymbol{\Delta}}(\mathbf{q})$ is continuous: The basic ECTM, which is represented by the $\text{sim}(\boldsymbol{\Delta}, \boldsymbol{\Sigma})$ function, constitutes a continuous mapping of demands on flows because it consists of a sequence of continuous flow updates. For a continuous demand constraint function $\widehat{\boldsymbol{\Delta}}(\mathbf{q})$, the combined function $\text{sim}(\min\{\boldsymbol{\Delta}, \widehat{\boldsymbol{\Delta}}(\mathbf{q})\}, \boldsymbol{\Sigma})$ is therefore continuous with respect to $\mathbf{q}$. This function maps every flow $\mathbf{q}$ in the closed, bounded, and convex set $\mathbf{0} \leq \mathbf{q} \leq \boldsymbol{\Delta}$ on this very set. That is, the model (13) specifies a fixed point of a continuous mapping of a closed, bounded, and convex set on itself. Brouwer's fixed point theorem guarantees that this mapping has at least one fixed point (Sobolev, 2001).

This model exhibits an important difference to the approach of van Hinsbergen et al. (2009) mentioned in the introduction. The latter replaces the demand constraint function $\widehat{\boldsymbol{\Delta}}(\mathbf{q})$ by a constraint function $\widehat{\boldsymbol{\Delta}}(\boldsymbol{\Delta})$ that does not depend on the actual flows $\mathbf{q}$ in the intersection but on the flow demands $\boldsymbol{\Delta}$. This has two implications:

1. Computations become easier because the demands $\boldsymbol{\Delta}$ are known before the flow calculations that depend on $\widehat{\boldsymbol{\Delta}}(\boldsymbol{\Delta})$. The specification $\widehat{\boldsymbol{\Delta}}(\mathbf{q})$ presented here requires to solve the unconstrained ECTM and the endogenous constraints in mutual dependency.

2. There are simple situations where $\widehat{\boldsymbol{\Delta}}(\boldsymbol{\Delta})$ fails. Assume an upstream demand Δ_1 that affects some other upstream demand Δ_2 via $\widehat{\Delta}_2(\Delta_1)$. Now, assume any situation where the actually transmitted portion of Δ_1 becomes arbitrarily small, e.g., because of a congested downstream cell or because of an interaction with another traffic stream. In the most extreme case, nothing of Δ_1 is transmitted at all such that its impact on the intersection effectively vanishes – but $\widehat{\Delta}_2(\Delta_1)$ invariably implies the same effect as if all of Δ_1 actually entered the intersection.

The approach of van Hinsbergen et al. (2009) is attractive because of its simplicity whenever replacing $\widehat{\boldsymbol{\Delta}}(\mathbf{q})$ by $\widehat{\boldsymbol{\Delta}}(\boldsymbol{\Delta})$ is feasible. However, this feasibility needs to be ascertained a priori for all possible congestion regimes of

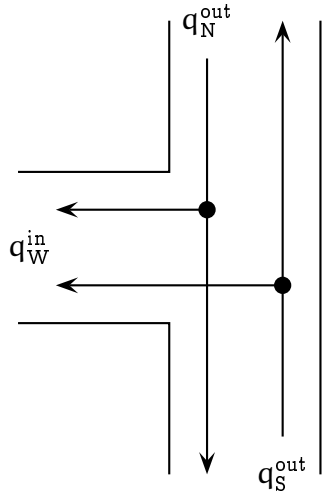

Figure 4: Simplified test network

A three-armed intersection, where some of flow q_N^{out}, coming from the north, turns into the westbound link and the remainder continues southbound. A portion of flow q_S^{out}, coming from the south, also turns into the westbound link, while the remainder continues northbound. The left-turning share of q_S^{out} yields to the southbound share of q_N^{out}. Traffic is single-lane in every direction.

an intersection, and, as the above example shows, it cannot be ascertained in general.

4.2 Uniqueness analysis

By incorporating endogenous constraints in the ECTM, two models are connected: The basic ECTM is, like the CTM, designed to identify the unique physically relevant solution of the KWM, given the CTM's basic phenomenological assumptions. The endogenous constraint function $\widehat{\mathbf{\Delta}}(\mathbf{q})$ is defined in a unique manner as well. However, without further assumptions there is no guarantee that the combined model (13) also has a unique solution. In this section, it is demonstrated that non-uniqueness is likely to result from misspecifications that are intimately related to the limitations of point-like intersection models as such.

Consider the situation shown in Figure 4. This is a three-armed intersection, where a fraction β_{NW} of flow q_N^{out}, coming from the north, turns into

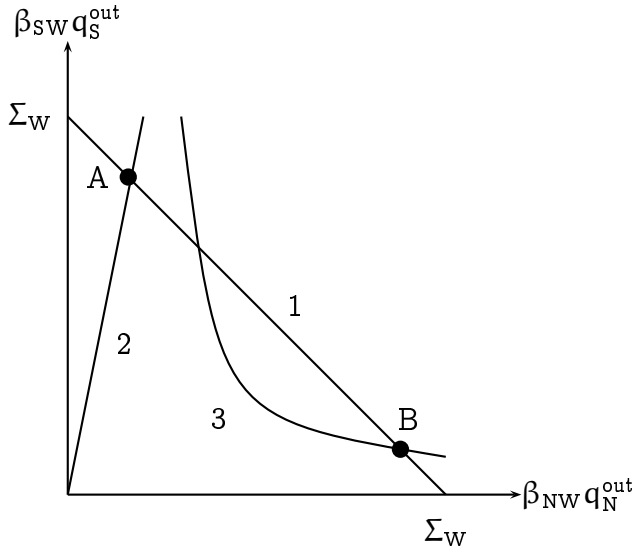

Figure 5: Ambiguous intersection flows

Given this constellation of the merge constraint 1, the priority constraint 2, and the endogenous flow constraint 3, there are two possible flow solutions A and B for the intersection of Figure 4.

the westbound link W and the remainder continues southbound. A fraction β_{SW} of flow q_S^{out}, coming from the south, also turns into link W, while the remainder continues northbound. The left-turning share of q_S^{out} yields to the southbound share of q_N^{out}. Traffic is single-lane in every direction. This is a simplified version of the previously used test network, where the minor stream coming from the east is removed for greatest clarity.

To begin with, the yielding of the left-turning flow is ignored and it is assumed that the flow supply Σ_W of the westbound link is the limiting factor of the intersection's throughput and that neither the demand Δ_N nor the demand Δ_S can be fully served such that

$$\beta_{NW} q_N^{out} + \beta_{SW} q_S^{out} = q_W^{in} = \Sigma_W. \tag{14}$$

This relation is represented by line 1 in Figure 5. Given the priorities α_N and α_S for the two ingoing streams,

$$\frac{\beta_{SW} q_S^{out}}{\beta_{NW} q_N^{out}} = \frac{\alpha_S}{\alpha_N} \tag{15}$$

holds furthermore in these conditions. An exemplary instance of this relation is given by line 2. Its intersection with line 1 at point A constitutes

the unique flow solution of the unconstrained intersection model.

Now, let the left-turning portion of q_S^{out} yield to the straight portion of q_N^{out}. The according endogenous flow constraint $\widehat{\Delta}_S(q_N^{out})$ is represented by curve 3 in Figure 5. A feasible flow solution must not be located above this curve. Point A maintains to be a feasible solution of the constrained model because the endogenous constraint is not violated. However, an inspection of point B now reveals the following properties: (i) given the transmitted flows, the endogenous constraint binds but is not violated, and (ii) a transmission of the accordingly constrained demands results in a situation that reproduces the endogenous constraint.

That is, both A and B are fixed points of (13), and hence both solve the intersection model. The cause of this ambiguity is the priority specification: Line 2 has a very large slope of α_S/α_N, which implies that q_S^{out} precedes q_N^{out} in the westbound merge. On the other hand, the endogenous flow constraint indicates the opposite: The left-turning portion of q_S^{out} yields to the southbound part of q_N^{out}. If the priorities were selected such that line 2 was flat enough to intersect curve 3 before reaching line 1, then point B would be the unique solution. Furthermore, if the slope of line 2 was so low that it intersected line 1 below point B, then only this new intersection point would solve the model.

The non-uniqueness in this example clearly results from a misspecified model. This type of misspecification is not easy to identify automatically, which is demonstrated by a slight modification of the intersection setting. Consider the modified version of the previous example shown in Figure 6. The only difference is that q_N^{out} is now allowed to u-turn and merge into the northbound part of q_S^{out}. A realistic priority rule for this setting would be that the the u-turning stream yields to the straight stream. This can lead to a situation where the endogenous constraint on the left-turning portion of q_S^{out} becomes inactive because the u-turning stream is held back such that it blocks the q_N^{out} stream, which otherwise would constrain q_S^{out}. This situation yields a flow diagram that looks qualitatively identical to Figure 5, only that line 1 now represents the new merge constraint of the northern intersection leg and line 2 represents the priorities at this merge. In this case, the correct solution is indeed represented by point A and not by point B.

Considering the wealth of intersection models that is enabled by removing

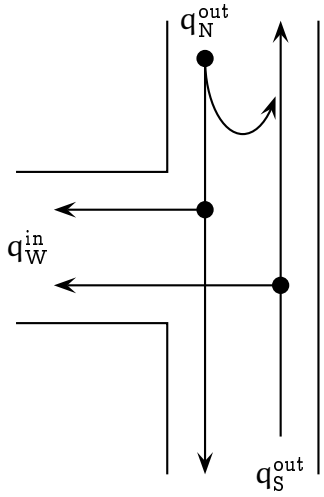

Figure 6: Simplified test network with additional u-turn
The only difference to the intersection of Figure 4 is that the traffic coming from the north is now allowed to u-turn and merge into the straight northbound stream.

the topology constraints of the original CTM, a unique specification that goes without additional modeling assumptions seems impossible to obtain. This is so because the generality of the ECTM reaches the limitations of what situations can be reasonably modeled by point-like intersections. If, for a very complex intersection, the spatial arrangement of interactions contains information that is necessary for a consistent models specification, then this intersection should indeed be modeled spatially, e.g., by linking several point-like intersection components. However, this statement does not invalidate the observation that an ECTM with well-modeled endogenous capacity constraints greatly improves the applicability of the original CTM.

4.3 Solution algorithms

The previous analysis shows that there may be multiple solutions of model (13), but it also indicates that such situations are likely to result from misspecifications. In this section, we present two solution procedures that both generate unique results with only a limited amount of computations.

In general, the difficulty of solving (13) has two major aspects.

1. Without further assumptions about the endogenous constraints, flows and constraints may be mutually dependent.

2. Different endogenous constraints may be mutually dependent as well because they are coupled through the flows.

These observations require a careful interpretation. At first glance, item 1 may give the impression that using the ECTM as a base model introduces additional complexity. Would it not be easier to entirely discard the ECTM and to return to a basic demand/supply framework in which all intersection phenomenology (including the merge logic) is modeled through constraints? Item 2 answers this question negatively.

In general, even the endogenous constraints cannot be treated independently. Consider, for example, the network shown in Figure 3. The minor stream coming from the east yields to both major streams. However, the left-turning portion of the major stream coming from the south also yields to the straight portion of the major stream coming from the north. That is, the constraint on the major stream generates flows changes that affect the constraint on the minor stream. Many situations of this type can be constructed, which shows that the difficult interactions of flows and constraints in model (13) are not a consequence of using the unconstrained ECTM as a base model but are an intrinsic feature of all point-like intersection models. Indeed, the basic ECTM even is of computational advantage because it already incorporates a complete set of merge constraints in a flow-transmission logic that terminates after a limited number of stages at an exact solution of the merge model.

In the following, two solution approaches to the fixed point problem (13) are described. Both approaches generate unique solutions and terminate after a limited number of calculations. The first approach yields an exact solution but requires an independence assumption to be satisfied. The second approach is universally applicable but yields only an approximate solution. For notational simplicity, it is assumed that every upstream outflow $i = 1 \dots I$ is subject to an endogenous constraint.

Exact solution procedure. Assume that the upstream outflows $i = 1 \dots I$ can be ordered such that outflow i is independent of all outflows

Algorithm 2 Exact solution procedure

1. $\mathbf{q}(0) = \text{sim}(\boldsymbol{\Delta}, \boldsymbol{\Sigma})$
2. $\boldsymbol{\Delta}' = \boldsymbol{\Delta}$
3. for $i = 1 \dots I$, do:
   (a) $\Delta'_i = \min\{\Delta_i, \widehat{\Delta}_i(\mathbf{q}(i-1))\}$
   (b) $\mathbf{q}(i) = \text{sim}(\boldsymbol{\Delta}', \boldsymbol{\Sigma})$
4. $\mathbf{q} = \mathbf{q}(I)$

$i+1 \dots I$ in terms of both the basic ECTM and the endogenous constraints. (This ordering is not unique if there are mutually independent outflows.) Then, (13) can be solved in I iterations by Algorithm 2.

First, the basic ECTM is run without constraints, which yields the flows $\mathbf{q}(0)$. Based on this, the highest ranking demand $i = 1$ is reduced according to the endogenous constraint $\widehat{\Delta}_1(\mathbf{q}(0))$. By assumption, this constraint will not change in reaction to variations in the outflows of $i = 2 \dots I$. Then, the basic ECTM is run again, using the constrained demand of $i = 1$, which yields the flows $\mathbf{q}(1)$. Because of the independence assumption, the constraint on $i = 1$ binds exactly in this and all following iterations. Now, the demand of $i = 2$ is constrained by $\widehat{\Delta}_2(\mathbf{q}(1))$, the ECTM is run again, and so forth. After I iterations, all constraints are satisfied, and the simulated flows reproduce these constraints.

Approximate solution procedure. If no ranking of the upstream outflows is possible because of mutual dependencies, Algorithm 3 can be deployed. It yields an approximate solution of the endogenously constrained simulation problem based on only two evaluations of the ECTM, between which it interpolates both the flows and the constraints. Note that this procedure can also be deployed as a building block in a more precise iterative solution algorithm.

The steps 1 and 2 identify the two working points A and B between the flows and the constraints are interpolated. Step 1 calculates the uncon-

Algorithm 3 Approximate solution procedure

1. calculate working point A:
   (a) $\mathbf{q}^A = \text{sim}(\boldsymbol{\Delta}, \boldsymbol{\Sigma})$
   (b) $\widehat{\boldsymbol{\Delta}}^A = \min\{\boldsymbol{\Delta}, \widehat{\boldsymbol{\Delta}}(\mathbf{q}^A)\}$
2. calculate working point B:
   (a) $\mathbf{q}^B = \text{sim}(\widehat{\boldsymbol{\Delta}}^A, \boldsymbol{\Sigma})$
   (b) $\widehat{\boldsymbol{\Delta}}^B = \min\{\boldsymbol{\Delta}, \widehat{\boldsymbol{\Delta}}(\mathbf{q}^B)\}$
3. solve linearized model with $\mathbf{q}(\lambda) = \mathbf{q}^B + \lambda(\mathbf{q}^A - \mathbf{q}^B)$ and $\widehat{\boldsymbol{\Delta}}(\lambda) = \widehat{\boldsymbol{\Delta}}^B + \lambda(\widehat{\boldsymbol{\Delta}}^A - \widehat{\boldsymbol{\Delta}}^B)$:
   (a) for all $i = 1 \ldots I$, evaluate

$$\lambda_i^* = \begin{cases} 1 & \text{if } \widehat{\Delta}_i^A = q_i^A \text{ and } \widehat{\Delta}_i^B = q_i^B \\ \dfrac{(\widehat{\Delta}_i^B - q_i^B)}{(\widehat{\Delta}_i^B - q_i^B) - (\widehat{\Delta}_i^A - q_i^A)} \rightarrow [0,1] & \text{otherwise} \end{cases}$$

   (b) $\lambda^* = \min_i \lambda_i^*$
   (c) $\mathbf{q} = \mathbf{q}^B + \lambda^*(\mathbf{q}^A - \mathbf{q}^B)$

strained flows A and the constraints A that result from these flows. Step 2 then calculates the flows B given the constraints A and identifies the new constraints B that result from the flows B. Step 3 solves the intersection model based on linearly interpolated flows and constraints. In particular, step 3a identifies for every upstream cell i the interpolation coefficient λ_i^* at which i's constraint binds. If a constraint bind at either working point, flow A, which effectively ignores the constraints, is assumed, which corresponds to $\lambda_i^* = 1$. Otherwise, λ_i^* results from equating the linearized flow and its constraint, solving for λ_i^*, and ensuring that no extrapolation takes place by projecting lambda on the interval $[0, 1]$. Step 3b then ensures that all constraints are simultaneously satisfied by the interpolated flows calculated in step 3c.

The consideration only of truly interpolated flows and constraints, i.e., the limitation of λ^* to $[0, 1]$, is justified by the observation that both working points constitute extreme cases of the model: Point A represents maximum flows because no endogenous constraints are applied. Assuming that increasing the flows in an intersection causes more mutual obstructions and hence a tightening of the endogenous constraints, point A also represents the tightest possible constraints. Vice versa, point B, resulting from these tightest constraints, represents particularly small flows B, which in turn result in extremely weak constraints B.

The following section applies both solution procedures to a non-trivial intersection model and compares the results to those obtained with a detailed traffic microsimulator.

4.4 Experimental results

The same network as used in Section 3.3 is considered, cf. Figure 3.

The ECTM is now supplemented with two endogenous flow constraints: One constraint affects the left-turning fraction of the northbound major stream because of the oncoming southbound major stream, and the second constraint affects the minor stream, which crosses both major streams. The ECTM's realism is evaluated through a comparison with the detailed traffic microsimulator AIMSUN NG 5.1.10 (TSS Transport Simulation Systems, 2006). The goal of this experiment is to investigate to what extent the ECTM is able to capture the microscopic vehicle interactions in the intersection at the macroscopic level and how well it reproduces the respective aggregate traffic characteristics.

All modeling assumptions described in Section 3.3 are maintained. The following ECTM parameters are obtained by manual calibration against the microsimulator, where the calibration objective is to minimize the deviations in simulated delays: All links but the minor street's entry link have a free flow speed of 50 km/h, a flow capacity of 2340 veh/h, a backward wave speed of 16 km/h, and a maximum density of 200 veh/km. The minor street's entry is stop-controlled. AIMSUN captures the effect of the stop sign by physically simulating a full stop of every vehicle in the minor stream. In the ECTM, this is reflected by choosing a flow capacity of 518 veh/h and a maximum velocity of 32.4 km/h (whereas the free flow speed in AIMSUN

is 50 km/h). The backward wave speed and the maximum density are the same as for all other links.

The links of the major street are 150 m long; the links of the minor street have a length of 100 m. All streets are modeled in AIMSUN as 1-lane urban roads (volume delay function 38786: VDF 25). The AIMSUN traffic demand consists of the vehicle type "car" only. For all microscopic vehicle parameters (e.g., maximum acceleration and deceleration, minimum distance between vehicles, etc.) the AIMSUN default values are chosen.

The demand inflow patterns are shown in Figure 7, where the bold lines represent macroscopic values in the ECTM and the thin lines are the according AIMSUN flows, which are averaged over 10 simulations but still exhibits substantial vehicle discretization noise. In AIMSUN, the inflow patterns are generated by adding traffic light controlled links upstream of each ingoing link of the original network (cycle time 90 s, major street: green time 24 s, minor street: green time 9 s). In the ECTM, piecewise linear demand flow patterns are found to reflect the AIMSUN inflows well. The figure clearly reflects the 90 s cycle time of the upstream traffic lights, which all turn green towards the central intersection at the same time. Furthermore, the constellation of link lengths, maximum velocities, and stop sign-induced delay is such that all platoons reach the intersection after approximately 11 s.

The two endogenous flow constraints in the ECTM are modeled in the following way.

- The left-turning portion of the northbound stream yields to the straight portion of the southbound stream. The demand constraint function capturing this effect is obtained from the German Highway Capacity Manual, Chapter "Unsignalized Intersections" (Forschungsgesellschaft für Strassen und Verkehrswesen, 2001). Its functional form is

$$\widehat{\Delta}_S(q_N^{out}) = \frac{1}{t_{f,S}} \exp\left[-q_N^{out}\left(t_{g,S} - \frac{t_{f,S}}{2}\right)\right] \tag{16}$$

  where q_N^{out} is flow rate of the southbound stream, $t_{g,S}$ is the minimum time gap between two southbound vehicles that allows one left-turning vehicle to enter the intersection, and $t_{f,S}$ is the minimum follow-up time between two left-turning vehicles. Both parameters

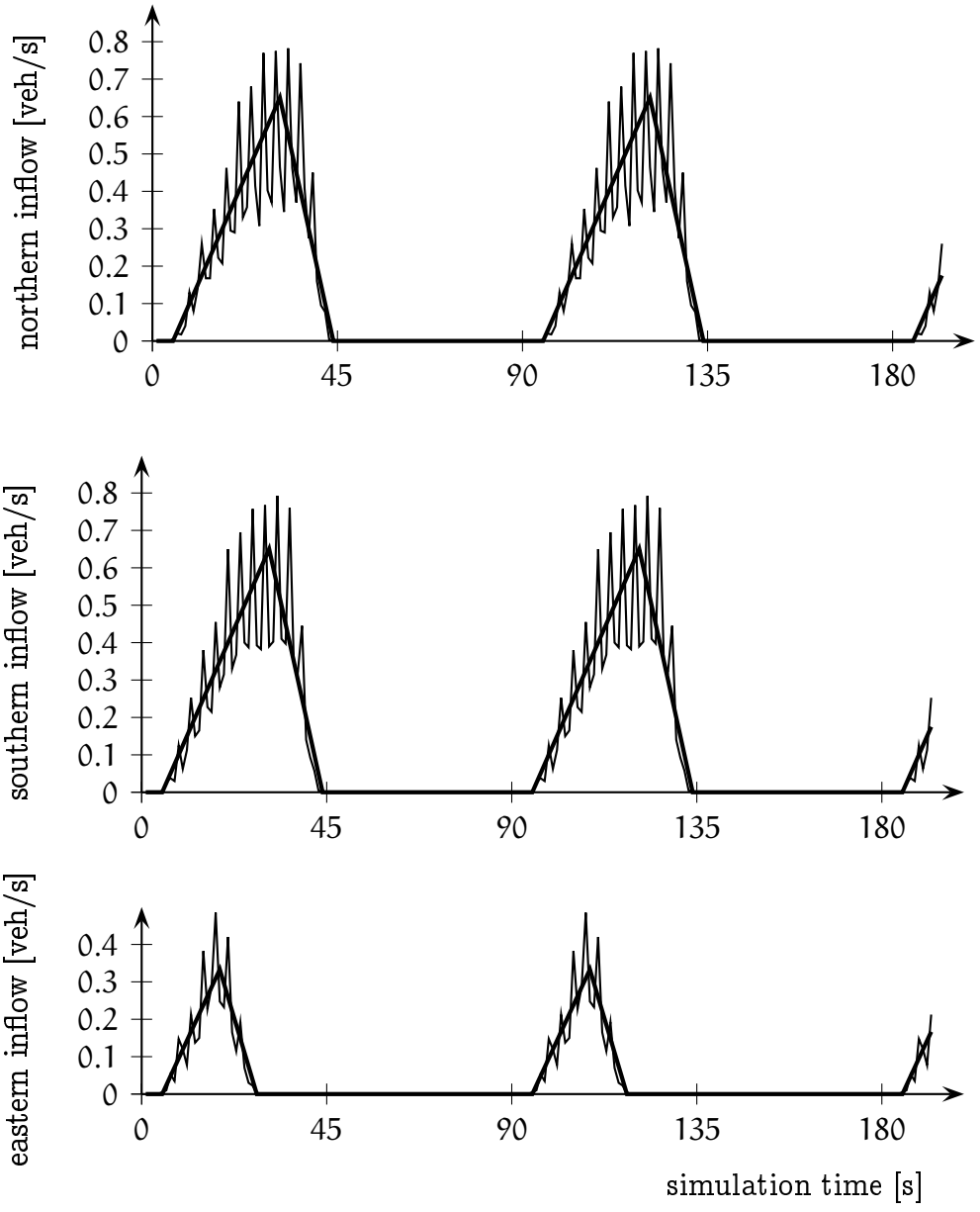

Figure 7: Comparison of AIMSUN and ECTM demand curves

The figure contains three diagrams, one for each ingoing link of the intersection. The thin noisy curve is the microscopic AIMSUN demand, and the respective fat smooth curve is the macroscopic ECTM demand. The AIMSUN curve is averaged over 10 runs of the microsimulator but still exhibits substantial vehicle discretization noise.

are identified by manual calibration against AIMSUN: $t_{g,S} = 8.4\,s$ and $t_{f,S} = 5.2\,s$.

- The minor road is stop-controlled and yields to the major streams. The effect of having to stop at all is captured by choosing a relatively small flow capacity and a small maximum velocity as described before. Beyond this, the minor stream yields to the major streams. The according demand constraint function is again obtained from (Forschungsgesellschaft für Strassen und Verkehrswesen, 2001):

$$\widehat{\Delta}_E(q_S^{out}, q_N^{out}) = \frac{p_{0,S}}{t_{f,E}} \exp\left[-(q_S^{out} + q_N^{out})\left(t_{g,E} - \frac{t_{f,E}}{2}\right)\right] \qquad (17)$$

  where $t_{g,E}$ and $t_{f,E}$ are again the minimum gap and the follow up time, q_S^{out} and q_N^{out} are the conflicting major flow rates, and $p_{0,S}$ is the probability that the left-turning traffic on the major street operates in a queue-free state. Again, the parameters are identified by manual calibration: $t_{g,E} = 9\,s$, $t_{f,E} = 8\,s$, and $p_{0,S} = 0.15$.

The chosen setting is such that the capacity of the westbound merge has no limiting effect on the intersection's flow throughput, which allows to explain all flow interactions by the endogenous constraints. This also enables a comparison of the exact and the approximate solution procedure for the ECTM, cf. Section 4.3: The constraints follow a hierarchical ordering (flow from the north precedes all other flows, flow from the south precedes flow from the east) such that the exact solution procedure can be applied. The approximate solution method is always feasible.

Figure 8 shows the simulation results for both AIMSUN and the ECTM. The figure contains three diagrams, one for each ingoing link's flow discharge into the intersection. The thin noisy curve is the AIMSUN output, which is averaged over 10 simulations, and the respective fat smooth curve is obtained from the ECTM (where the exact and the approximate solution procedure yield visually identical results). We begin by describing the general phenomenology of the intersection as it is captured by both models.

Cars coming from the north traverse the intersection without interruption. One observes a shift of the respective demand profile by approximately 11 s, which is the time it takes the demand to travel from the network entry to the central intersection. The flow coming from the south is equally

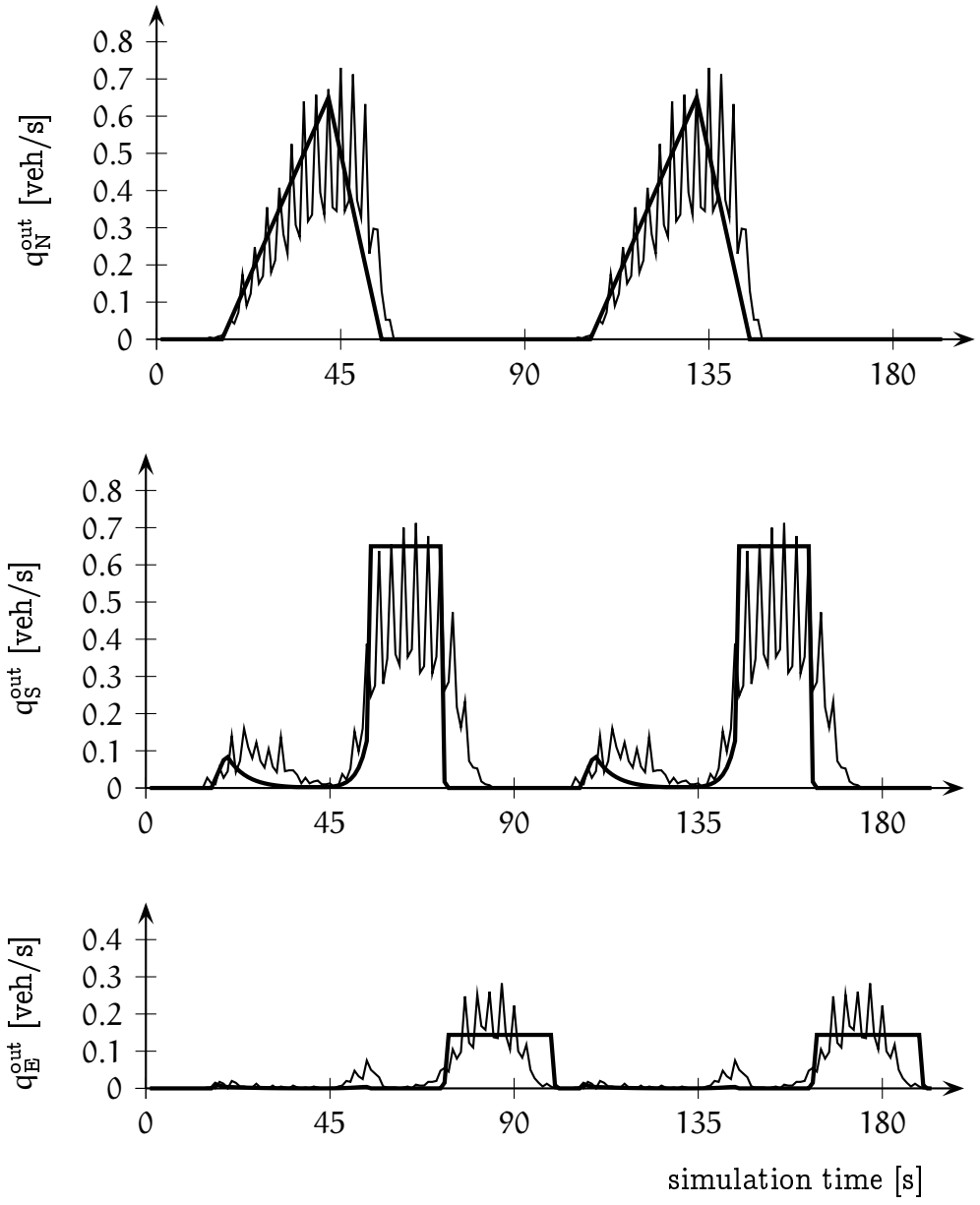

Figure 8: Comparison of AIMSUN and ECTM simulation results
The figure contains three diagrams, one for each ingoing link of the intersection. The thin noisy curve is the AIMSUN output, and the respective fat smooth curve is obtained from the ECTM. The AIMSUN curve is averaged over 10 runs of the microsimulator but still exhibits substantial vehicle discretization noise.

delayed, but once it reaches the intersection, its left-turning portion is quickly suppressed by the prior-ranking southbound flow, which effectively holds up the entire northbound flow (remember that all roads have a single lane only). Only when the southbound flow ceases, the northbound flow can continue, which it does at maximum capacity. Finally, the minor stream going from east to west is held up until both major streams have passed the intersection. Some minor flow makes it through when the southbound flow ceases and the northbound flow has not yet reached its maximum value. All queues recover within a 90 s cycle.

A comparison between AIMSUN and the endogenously constrained ECTM shows that the microscopic traffic phenomena (no interruption of the southbound flow; temporary queuing of both other flows) are well captured by the macroscopic model. The uninterrupted outflow from the north is somewhat wider in AIMSUN than in the ECTM because the latter does not capture platoon dispersion, which, however, is not so much of an intersection modeling problem but rather an inherent features of all first order models.[2] The endogenous constraints generate flow reductions that are consistent with AIMSUN's representation of the respective vehicle interactions. The recovery of the southern queue is faster in the ECTM than in the microsimulator because the KWM postulates infinite vehicle accelerations. This, again, is an inherent feature of all first order models.

The visual impression of the flow curves presented above is supported by a quantitative comparison of the average densities and delays on all links in the network. The results are shown in Table 3 and exhibit a remarkable accuracy. In particular, the delay estimates of the ECTM almost perfectly reproduce the outputs of the far more complicated microsimulator. It also is noteworthy that the exact and the approximate solution procedure yield almost identical results.

These experiments give clear indication that the endogenously constrained ECTM captures the flow interactions in complex intersections very well.

[2] Dispersion at the downstream end of a platoon could be captured by choosing a truly concave flow demand function Δ. Dispersion at a platoon's upstream end, however, cannot be captured by a first order model: Flows at lower densities are never slower than flows at higher densities such that any platoon tail will eventually catch up with the platoon main body and transform into a density discontinuity at its upstream end.

Table 3: Quantitative comparison of ECTM and AIMSUN

link	density [veh/km]			delay [s/veh]		
	AIM-SUN	ECTM (exact)	ECTM (approx.)	AIM-SUN	ECTM (exact)	ECTM (approx.)
S, ingoing	28.6	31.7	31.6	23	23	23
E, ingoing	24.5	29.3	29.2	59	57	56
N, ingoing	11.7	10.1	10.1	3	0	0
N, outgoing	4.5	4.9	4.9	1	0	0
W, outgoing	14.5	13	13	1	0	0
S, outgoing	4.7	5	5	1	0	0

5 Summary

This article demonstrates that the extended cell-transmission model (ECTM) is well applicable to the modeling of complex intersections from a methodological, computational, and practical point of view.

Methodologically, the proposed model is founded on two elements: the original CTM's phenomenology and the framework of flow demands and supplies. The CTM is extended towards intersections of general topology while preserving its relevant phenomenological features. The resulting ECTM inherits the CTM's minimal flow constraints, which alone is insufficient to model urban intersections with substantial stream-line interactions. However, the ECTM does constitute a flexible base model that can be adopted to a particular application by adding supplementary flow constraints. For this purpose, a fixed point formulation of the ECTM with supplementary flow constraints is presented, and it is demonstrated that the uniqueness of this formulation depends on a phenomenologically consistent model specification. This result carries over to arbitrary intersection models that implement the demand/supply framework.

Computationally, two efficient solution procedures for the fixed point model formulation are presented. The first approach is exact but assumes that all intersection inflows can be ordered in some priority-related manner, whereas the second approach applies to arbitrary intersections but yields only approximate solutions. Both procedures perform very well in comparison with a detailed traffic flow microsimulator.

Practically, an incremental modeling procedure is enabled that builds on the unconstrained ECTM and adds further flow constraints only if necessary. Since the CTM, from which the ECTM is derived, is well-understood and requires only a low number of intuitive parameters, this approach is practically appealing. The experiments show that good results can be achieved even when only the most obvious constraints are added to the ECTM.

6 Acknowledgments

Peter Wagner provided very helpful comments on this article.

References

R. Ansorge (1990). 'What does the entropy condition mean in traffic flow theory'. *Transportation Research Part B* **24**(2):133–143.

V. Astarita, et al. (2001). 'A comparison of three methods for dynamic network loading'. *Transportation Research Record* **1771**:179–190.

M. Ben-Akiva, et al. (2001). 'Network state estimation and prediction for real–time transportation management applications'. *Networks and Spatial Economics* **1**:293–318.

M. Brackstone & M. McDonald (1999). 'Car-following: a historical review'. *Transportation Research Part F* **2**(4):181–196.

E. Brockfeld & P. Wagner (2006). 'Validating microscopic traffic flow models'. In *Proceedings of the 9th IEEE Intelligent Transportation Systems Conference*, pp. 1604–1608, Toronto, Canada.

C. Buisson, et al. (1996a). 'STRADA. A discretized macroscopic model of vehicular traffic flow in complex networks based on the Godunov scheme.'. In *Symposium on Modelling, Analysis and Simulation, held at CESA 1996 IMACS Multiconference*, vol. 2, pp. 976–981, Lille, France.

C. Buisson, et al. (1996b). 'The STRADA model for dynamic assignment'. In *Proceedings of the 1996 ITS Conference*, Orlando, USA.

R. Chrobok, et al. (2003). 'Traffic forecast using a combination of on-line simulation and traffic data'. In M. Fukui, Y. Sugiyama, M. Schreckenberg, & D. Wolf (eds.), *Traffic and Granular Flow '01*, pp. 345–350. Springer.

C. Daganzo (1994). 'The cell transmission model: a dynamic representation of highway traffic consistent with the hydrodynamic theory'. *Transportation Research Part B* **28**(4):269–287.

C. Daganzo (1995a). 'The cell transmission model, part II: network traffic'. *Transportation Research Part B* **29**(2):79–93.

C. Daganzo (1995b). 'A finite difference approximation of the kinematic wave model of traffic flow'. *Transportation Research Part B* **29**(4):261–276.

C. Daganzo (2006). 'In traffic flow, cellular automata = kinematic waves'. *Transportation Research Part B* **40**(5):396–403.

A. De Palma & F. Marchal (2002). 'Real cases applications of the fully dynamic METROPOLIS tool-box: an advocacy for large-scale mesoscopic transportation systems'. *Networks and Spatial Economics* **2**:347–369.

O. Feldman & M. Maher (2002). 'The optimisation of traffic signals using a cell transmission model'. In *Proceedings of the 9th Meeting of the EURO Working Group on Transportation*, pp. 503–507, Bari, Italy.

G. Flötteröd (2008). *Traffic State Estimation with Multi-Agent Simulations*. Ph.D. thesis, Berlin Institute of Technology, Berlin, Germany.

G. Flötteröd & K. Nagel (2005). 'Some practical extensions to the cell transmission model'. In *Proceedings of the 8th IEEE Intelligent Transportation Systems Conference*, pp. 510–515, Vienna, Austria.

Forschungsgesellschaft für Strassen und Verkehrswesen (2001). *Handbuch für die Bemessung von Strassenverkehrsanlagen*. FSGV Verlag GmbH, Köln.

B. Friedrich & E. Almasri (2006). 'A new method for offset optimization in urban road networks'. In *Proceedings of the 11th Meeting of the Euro Working Group Transportation*, Bari, Italy.

B. Greenshields (1935). 'A study of traffic capacity'. In *Proceedings of the Annual Meeting of the Highway Research Board*, vol. 14, pp. 448–477.

S. Hoogendoorn & P. Bovy (2001). 'State-of-the-art of vehicular traffic flow modelling'. *Proceedings of the Institution of Mechanical Engineers. Part I: Journal of Systems and Control Engineering* **215**(4):283–303.

W. Jin & H. Zhang (2003). 'On the distribution schemes for determining flows through a merge'. *Transportation Research Part B* **37**(6):521–540.

J. Lebacque (1996). 'The Godunov scheme and what it means for first order traffic flow models'. In J.-B. Lesort (ed.), *Proceedings of the 13th International Symposium on Transportation and Traffic Theory*, Lyon, France. Pergamon.

J. Lebacque & M. Koshyaran (2002). 'First order macroscopic traffic flow models for networks in the context of dynamic assignment'. In M. Patriksson & M. Labbé (eds.), *Transportation Planning*, pp. 119–139. Kluwer.

S. Lee (1996). 'A Cell Transmission Based Assignment-Simulation Model for Integrated Freeway/Surface Street Systems'. Master thesis, Ohio State University.

R. LeVeque (1992). *Numerical Methods for Conservation Laws*. Lectures in Mathematics: ETH Zürich. Birkhäuser.

M. Lighthill & J. Witham (1955). 'On kinematic waves II. A theory of traffic flow on long crowded roads'. *Proceedings of the Royal Society A* **229**:317–345.

H. S. Mahmassani (2001). 'Dynamic network traffic assignment and simulation methodology for advanced system management applications'. *Networks and Spatial Economics* **1**(3/4):267–292.

L. Munoz, et al. (2006). 'A piecewise-linearized cell transmission model and parameter calibration methodology'. In *Proceedings of the 85.*

Annual Meeting of the Transportation Research Board, Washington, DC, USA.

L. Munoz, et al. (2004). 'Methodological calibration of the cell transmission model'. In *Proceedings of the American Control Conference*, pp. 798–803, Denver, Colorado.

K. Nagel & P. Nelson (2005). 'A critical comparison of the kinematic-wave model with observational data'. In H. Mahmassani (ed.), *Proceedings of the 16th International Symposium on Transportation and Traffic Theory*, pp. 145–163, Maryland, USA. Elsevier.

K. Nökel & M. Schmidt (2002). 'Parallel DYNEMO: meso-scopic traffic flow simulation on large networks'. *Networks and Spatial Economics* **2**(4):387–403.

S. Pandawi & H. Dia (2005). 'Comparative evaluation of microscopic car-following behavior'. *IEEE Transactions on Intelligent Transportation System* **6**(3):314–325.

H. Payne (1971). 'Models of freeway traffic and control'. In *Mathematical Models of Public Systems*, vol. 1, pp. 51–61. Simulation Council, La Jolla, CA, USA.

P. Richards (1956). 'Shock waves on highways'. *Operations Research* **4**:42–51.

V. Sobolev (2001). 'Brouwer theorem'. In M. Hazewinkel (ed.), *Encyclopedia of Mathematics*. Kluwer.

X. Sun, et al. (2003). 'Highway traffic state estimation using improved mixture Kalman filters for effective ramp metering control'. In *Proceedings of the 42th IEEE Conference on Decision and Control*, pp. 6333–6338, Maui, Hawaii, USA.

C. Tampere & L. Immers (2007). 'An extended Kalman filter application for traffic state estimation using CTM with implicit mode switching and dynamic parameters'. In *Proceedings of the 10th IEEE Intelligent Transportation Systems Conference*, pp. 209–216, Seattle, USA.

TSS Transport Simulation Systems (2006). *AIMSUN 5.1 Microsimulator User's Manual Version 5.1.4*.

C. van Hinsbergen, et al. (2009). 'Urban intersections in first order models with the Godunov scheme'. In *Proceedings of mobil.TUM 2009 – International Scientific Conference on Mobility and Transport – ITS for large Cities*, Munich, Germany.

A. Ziliaskopoulos & S. Lee (1997). 'A cell transmission based assignment simulation model for integrated freeway/surface street systems'. In *Proceedings of the 76. Annual Meeting of the Transportation Research Board*, Washington, DC, USA.